Phys Chem Minerals (2000) 27: 575–582

ORIGINAL PAPER

J. Haines · J. M. Léger · C. Chateau · A. S. Pereira

Structural evolution of rutile-type and $CaCl_2$-type germanium dioxide at high pressure

Received: 30 September 1999 / Accepted: 27 February 2000

Abstract Germanium dioxide was found to undergo a transition from the tetragonal rutile-type to the orthorhombic $CaCl_2$-type phase above 25 GPa. The detailed structural evolution of both phases at high pressure in a diamond anvil cell has been investigated by Rietveld refinement using angle-dispersive, X-ray powder-diffraction data. The square of the spontaneous strain $(a-b)/(a+b)$ in the orthorhombic phase was found to be a linear function of pressure and no discontinuities in the cell constants and volume were observed, indicating that the transition is second-order and proper ferroelastic. Compression of the GeO_6 octahedra was found to be anisotropic, with the apical Ge-O distances decreasing to a greater extent than the equatorial distances and becoming shorter than the latter above 7 GPa. Above this pressure, the GeO_6 octahedron exhibits the common type of tetragonal distortion predicted by a simple ionic model and observed for most rutile-type structures such as those of the heavier group-14 dioxides and the metal difluorides. Above the phase transition, the columns of edge-sharing octahedra tilt about their two fold axes parallel to **c** and the rotation angle reaches 10.2(5)° by 36(1) GPa so as to yield a hexagonal close-packed oxygen sublattice. The compressibility increases at the phase change as is expected for a second-order transition at which an additional compression mechanism becomes available.

Key words Germanium dioxide · High pressure phase transition · Rietveld refinement

J. Haines (✉) · J. M. Léger · C. Chateau · A. S. Pereira
Laboratoire de physico-chimie des matériaux, CNRS, 1, Place Aristide Briand 92190 Meudon, France
e-mail: Haines@cnrs-bellevue.fr
Tel.: +33-1-45075511
Fax: +33-1-45075910

Permanent address:
A. S. Pereira
Instituto de Fisica and Escola de Engenharia, UFRGS, 91501-970 Porto Alegre, RS Brazil

Introduction

There has been a great deal of interest in the high-pressure phase transitions of stishovite rutile-type silica, due to the possible geophysical repercussions of such transitions. Among the dioxides, GeO_2 is the closest analog to silica, and thus the study of rutile-type GeO_2 may further the understanding of the high-pressure behavior of stishovite. Stishovite was found to undergo a phase transition from the tetragonal rutile-type $(P4_2/mnm, Z=2)$ to an orthorhombic, $CaCl_2$-type $(Pnnm, Z=2)$ phase by Raman spectroscopy (Kingma et al. 1995) and X-ray diffraction (Mao et al. 1994; Andrault et al. 1998) at pressures of between 50 and 56 GPa. Second-order rutile-type to $CaCl_2$-type transitions have also been observed in GeO_2 at 26.7 GPa by Raman spectroscopy (Haines et al. 1998) and in the heavier group-14 dioxides, SnO_2 (Haines and Léger 1997) and PbO_2 (Haines et al. 1996a), from X-ray diffraction measurements. Molecular dynamics calculations indicate a much higher transition pressure of 80 GPa for GeO_2 (Tsuchiya et al. 1998). Up to the present, there are no structural data for rutile-type GeO_2 above 7.2 GPa (Hazen and Finger 1981; Léger et al. 1998), which is well below the observed phase transition pressure. In the present study, the structural evolution of GeO_2 up to 36 GPa is described and compared with the behavior of stishovite and the other group-14 dioxides.

Experimental

Rutile-type GeO_2 was prepared from the quartz-type phase (Produits Touzart and Matignon, purity 99.999%) at 3 GPa and 585 °C in a belt-type apparatus. No impurities could be detected in the sample by X-ray diffraction, and the widths of the diffraction lines are consistent with a crystallite size of 70 nm.

High-pressure X-ray diffraction experiments were performed using a diamond anvil cell in which the rear diamond was mounted over a 16°-wide slit allowing access to $4\theta = 80°$. The powdered rutile-type GeO_2 was loaded in the 150-μm holes drilled in inconel gaskets preindented to a thickness of 100–120 μm. Several grains of

ruby powder were added as a pressure calibrant. In certain runs, up to 10% w/w titanium carbide or platinum was mixed with the sample in order to absorb laser radiation for heating. In the experiments, up to 16.1 GPa, 16:3:1 methanol:ethanol:water was used as a pressure-transmitting medium, whereas for higher pressures cryogenically loaded nitrogen was used. At all pressures above 11 GPa, laser heating was performed using a 50-W Nd-Yag laser in order to minimize deviatoric stress. The laser was slowly scanned over the sample for a period of typically 1–2 h. The temperature was not measured; however, the intensity of the visual emission produced from the 5-μm diameter hot spot indicated a temperature of the order of 1000 °C. The pressure was measured based on the shift of the ruby R_1 and R_2 fluorescence lines (Mao et al. 1986). In one run, in which 10% w/w TiC was added, yielding a very black sample mixture, the pressures estimated based on the ruby signals, which originated from the sample-mixture-diamond interface, proved to be unreliable. The ruby lines were very broad, indicating contact between the ruby and the diamond, whereas the diffraction lines remained sharp. In this run, the pressure was estimated based on the equation of state of titanium carbide with a bulk modulus of 242 GPa (Chang and Graham 1966) and a first pressure derivative of 4.

Angle-dispersive X-ray powder-diffraction data were obtained on an imaging plate placed at between 117.21 and 147.90 mm from the sample, using zirconium-filtered molybdenum radiation from a microfocus tube. These distances were measured mechanically with a precision of ±0.03 mm. Data were obtained either with a 130 × 130 μm beam defined using a collimator built of two sets of crossed slits, or using the 100-μm beam from an X-ray capillary optic. Exposure times were 48–60 h. An additional exposure was performed on the same installation at ambient pressure with a GeO_2 sample in a 0.3-mm diameter glass capillary and an imaging plate at a distance of 143.06 mm.

The observed intensities on the imaging plate were integrated as a function of 2θ in order to obtain conventional one-dimensional diffraction profiles. The resulting profiles were used for multiphase Rietveld refinement using the program FULLPROF (J. Rodríguez-Carvajal, unpublished) in order to account for lines from TiC, N_2, and nickel from the gasket in addition to GeO_2. In addition to the cell constants and atomic positional parameters for GeO_2, scale factors, line shape, and an overall thermal parameter were varied. Strain parameters were also included for GeO_2 near and above the phase transition to account for preferential broadening of certain diffraction lines due to fine-scale twinning effects. The inclusion of a preferred orientation parameter resulted in no improvement to the fits. This was taken as evidence that preferred orientation effects were absent. A similar absence was also observed for $CaCl_2$-type SnO_2 under hydrostatic conditions (Haines and Léger 1997). Due to the low diffracted intensity arising from ε-N_2, all values for this phase, except the scale factor, were fixed. A recent study of TiC at high pressure by Dubrovinskaia et al. (1999) indicated that a transition to a rhombohedral phase occurs above 18 GPa at ambient temperature. This transition was not observed in the present work on laser-annealed samples and no deviation from cubic symmetry was detected in the Rietveld refinements. Figures in parentheses refer to standard uncertainties given by FULLPROF in the case of diffraction data and estimated error for other measured values.

Results and discussion

Rutile-type to $CaCl_2$-type phase transition

The structure of rutile-type GeO_2 (Fig. 1) is composed of columns of edge-sharing GeO_6 octahedra lying along **c**, which are cross-linked along the [1 1 0] and [1 $\bar{1}$ 0] directions. In this structure, the oxygen array is tetragonal close-packed (Baur 1981; West and Bruce 1982; Wells and Chamberland 1987). This arrangement is slightly less dense than hexagonal close packing and can be described as a distorted puckered hexagonal closest packing. There is one refinable atomic positional parameter, the oxygen *x*-coordinate (Table 1). The value obtained in this study at ambient pressure of 0.3063(3) is in very good agreement with the values of 0.3059(2) and 0.3061(13) obtained using single-crystal X-ray diffraction (Baur and Khan 1971; Hazen and Finger 1981) and that of 0.30604(6) using neutron powder diffraction (Bolzan et al. 1997). The diffraction data obtained at pressures up to and including 25 GPa were consistent with a tetragonal rutile-type structure (Fig. 2; Table 1). At pressures between 28 and 36 GPa, the *hkl* ($h \neq k$) diffraction lines were found to split, whereas the *hhl* lines did not, indicating an orthorhombic distortion of the parent tetragonal structure. This is identical to what was observed at the rutile-type to $CaCl_2$-type transitions in a series of dioxides, SiO_2 (Andrault et al. 1998), SnO_2 (Haines and Léger 1997), PbO_2 (Haines et al. 1996a), MnO_2 (Haines et al. 1995), and RuO_2 (Haines and Léger

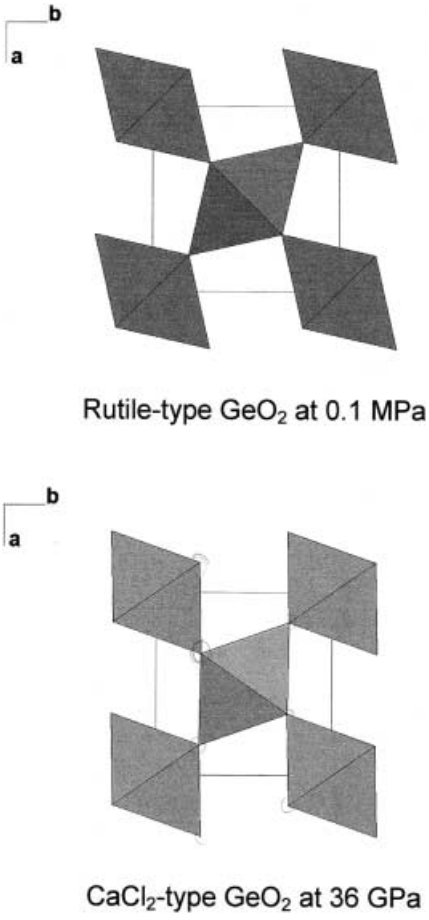

Fig. 1 Polyhedral representations of the crystal structures of rutile-type and $CaCl_2$-type GeO_2 projected on the *xy* plane. Note that the tilt angle of the GeO_6 octahedra by 10° with respect to their orientation in the rutile structure produces the hexagonal close-packed oxygen planes perpendicular to **b** in the $CaCl_2$-type structure shown *below*. In consequence, the oxygens no longer lie in the [1 1 0] and [1 $\bar{1}$ 0] planes

Table 1 Structural data for tetragonal rutile-type GeO_2 [$P4_2/mnm$, $Z = 2$, Ge^{4+} on 2*a* site (0, 0, 0) O^{2-} on 4*f* sites (*x*, *x*, 0)] and orthorhombic $CaCl_2$-type GeO_2 [*Pnnm*, $Z = 2$, Ge^{4+} on 2*a* site (0, 0, 0) O^{2-} on 4g sites (*x*, *y*, 0)]

P (GPa)[a]	*a* (Å)	*b* (Å)	*c* (Å)	*x*	*y*	$R_B/R_{wp}/R_p$ (%)[b]
Ambient	4.3966(1)	–	2.8626(1)	0.3063(3)	–	2.5/4.3/7.0
Ambient[c]	4.3964	–	2.8626	0.3061	–	
1.71[c]	4.3856	–	2.8598	0.3060	–	
3.19[c]	4.3752	–	2.8574	0.3047	–	
3.70[c]	4.3711	–	2.8558	0.3035	–	
4.2(1)	4.3751(1)	–	2.8511(1)	0.3048(4)	–	2.0/4.9/6.8
5.0(2)[d]	4.3666(1)	–	2.8522(1)	0.3047(3)	–	1.6/3.5/4.1
6.2(2)	4.3553(1)	–	2.8463(1)	0.3030(4)	–	3.0/5.4/7.9
7.2(2)[d]	4.3483(1)	–	2.8436(1)	0.3036(4)	–	2.3/4.7/7.0
8.9(3)	4.3417(1)	–	2.8407(1)	0.3027(4)	–	2.3/5.3/7.4
10.4(3)	4.3340(1)	–	2.8376(1)	0.3035(4)	–	2.0/4.8/7.2
10.5(3)	4.3349(1)	–	2.8424(1)	0.3029(6)	–	2.6/7.1/7.4
16.1(5)	4.2980(1)	–	2.8295(1)	0.2997(7)	–	3.1/6.9/7.4
20.3(9)	4.2835(2)	–	2.8193(2)	0.2985(5)	–	2.5/6.6/7.9
25(1)	4.2630(2)	–	2.8148(2)	0.2972(6)	–	2.3/7.6/10.7
28(1)	4.2841(9)	4.2098(9)	2.8089(3)	0.335(2)	0.264(2)	2.3/6.7/9.4
29(1)	4.2852(6)	4.1959(6)	2.8062(2)	0.335(2)	0.262(1)	2.2/5.6/7.4
32(1)	4.2866(6)	4.1742(6)	2.7995(3)	0.340(2)	0.256(1)	1.8/5.5/7.2
35(1)	4.2834(6)	4.1508(5)	2.7941(3)	0.336(2)	0.225(1)	1.4/5.6/7.0
36(1)	4.2814(6)	4.1424(6)	2.7919(3)	0.335(2)	0.255(1)	2.3/6.1/7.5

[a] Ruby fluorescence was used for pressure measurements below 20 GPa, whereas the equation of state of TiC was used above this pressure. It can be noted that above 20 GPa the average difference between the pressure given by the TiC and the ruby which was in contact with the diamond anvil was 1 GPa
[b] Agreement factor B = Bragg, p = profile, wp = weighted profile
[c] Single-crystal data (Hazen and Finger 1981)
[d] Powder data (Léger et al. 1988)

1993; Haines et al. 1997), and in the case of GeO_2, refinements could readily be performed using a $CaCl_2$-type structural model (Fig. 3; Table 1).

Landau theory predicts that a transition from a tetragonal rutile-type structure, space group $P4_2/mnm$ $Z = 2$, to an orthorhombic $CaCl_2$-type structure, space group $Pnnm$ $Z = 2$, should be second-order and proper ferroelastic and involve the softening of the Raman-active B_{1g} mode (Salje 1990; Stokes and Hatch 1988). This mode corresponds to a libration of the columns of GeO_6 octahedra about their two fold axes parallel to **c**. The Raman-active B_{1g} mode in rutile-type GeO_2 does indeed soften with pressure up to 26.7 GPa, above which it becomes a hard A_g mode (Haines et al. 1998). In the present X-ray diffraction study, the cell constants (Fig. 4) and volume (Fig. 5) exhibit no discontinuities as required for a second-order phase transition. The primary order parameter for this transition is the spontaneous strain, $e_{ss} = (a - b)/(a + b)$, which is of B_{1g} symmetry. As shown previously for this type of proper

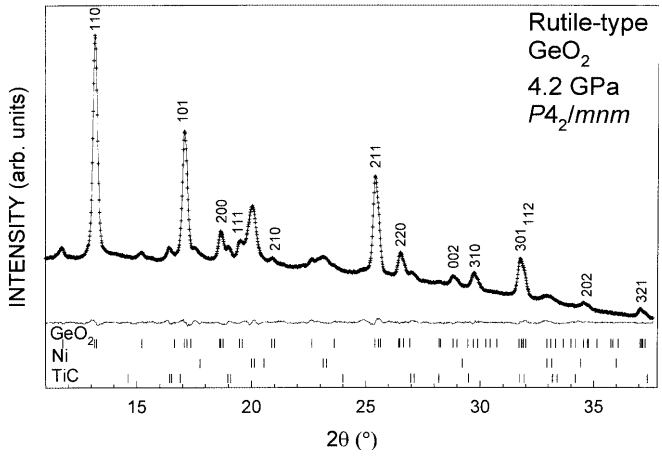

Fig. 2 Experimental data (+) and calculated profiles (*solid line*) from the Rietveld refinement of rutile-type GeO_2 at 4.2 GPa. Intensity is in arbitrary units and the difference profile is on the same scale. *Vertical bars* indicate the calculated positions of reflections ($\kappa\alpha_1$, $\kappa\alpha_2$, $\kappa\beta$) arising from GeO_2, Ni from the gasket and TiC. The diffraction lines of GeO_2 are *indexed*

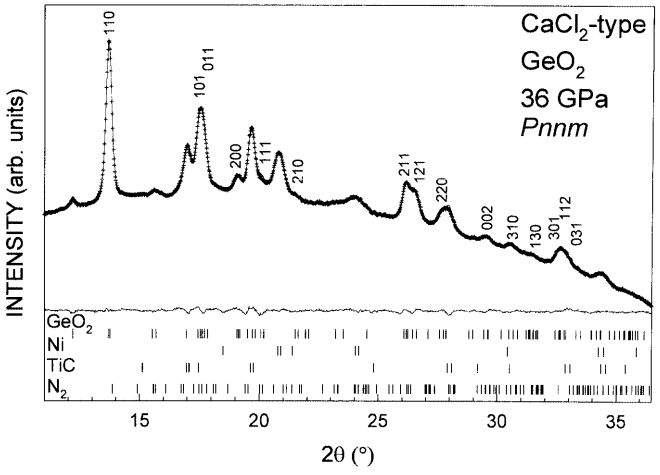

Fig. 3 Experimental data (+) and calculated profiles (*solid line*) from the Rietveld refinement of $CaCl_2$-type GeO_2 at 36 GPa. Intensity is in arbitrary units and the difference profile is on the same scale. *Vertical bars* indicate the calculated positions of reflections ($\kappa\alpha_1$, $\kappa\alpha_2$, $\kappa\beta$) arising from GeO_2, Ni from the gasket and TiC and ε-N_2. The diffraction lines of GeO_2 are *indexed*. Note the splitting of the tetragonal 211, 310, and 301 reflections in the 2θ range beyond 25°

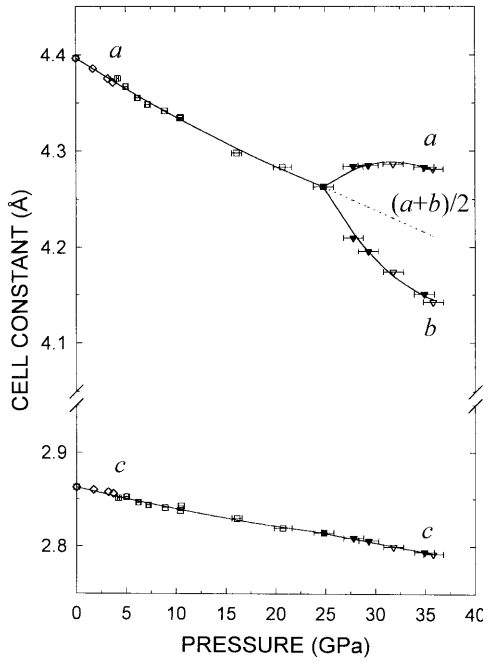

Fig. 4 Cell constants of rutile-type (□) and $CaCl_2$-type (▽) GeO_2 as a function of pressure. The single-crystal data of Hazen and Finger 1981 are indicated by ◊. *Lines* represent least-squares fits to the data. *Open* and *solid symbols* refer to points obtained on compression and decompression, respectively

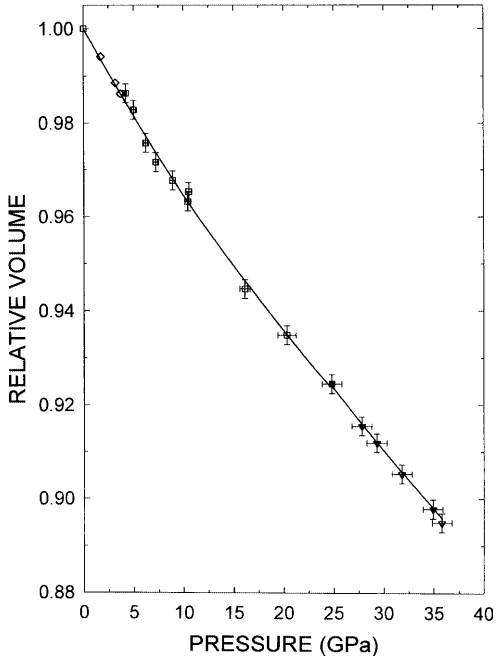

Fig. 5 Relative volume of rutile-type (□) and $CaCl_2$-type (▽) GeO_2 as a function of pressure. The single-crystal data of Hazen and Finger 1981 are indicated by ◊. *Lines* represent Birch-Murnaghan equations of state using the parameters given in the text. *Open* and *solid symbols* refer to points obtained on compression and decompression, respectively

ferroelastic transition (Haines and Léger 1993; Haines et al. 1995), the square of the spontaneous strain should be a linear function of $(P - P_c)$, where P_c is the critical pressure. This is indeed the case for GeO_2 and extrapolation of e_{ss}^2 gives a critical pressure of 25 ± 1 GPa (Fig. 6) in good agreement with the value obtained from Raman measurements (Haines et al. 1998). Preferential broadening of the *hkl* reflections which split in the orthorhombic phase, was observed in the present study, as was also the case for SnO_2 (Haines and Léger 1997) and MnO_2 (Haines et al. 1995). This broadening is an indication of the existence of fine-scale twinning commonly observed at ferroelastic transitions.

Compressibility and equation of state

The *P-V* data for GeO_2 were fitted using two Birch-Murnaghan equations of state (Birch 1947):

$$P = 1.5B_0[(V/V_0)^{-7/3} - (V/V_0)^{-5/3}]\{1 + 0.75(B_0' - 4) \times [(V/V_0)^{-2/3} - 1]\} \ , \quad (1)$$

where B is the bulk modulus and B' is its first pressure derivative. The subscript zero refers to the value at ambient pressure. A bulk modulus of 250(9) GPa with a B_0' of 5.6(9) was obtained from fitting the data for the rutile-type phase ($P \leq 25$ GPa) in Table 1 to the above equation. These values are in good agreement with the results of ultrasonic measurements (Wang and Simmons 1973), $B_0 = 259$ GPa with $B_0' = 6.16$, and with those obtained from molecular dynamics calculations (Tsuchiya et al. 1998), $B_0 = 245$ GPa with $B_0' = 4.7$). A fit to the data for the high-pressure $CaCl_2$-type phase ($P \geq 28$

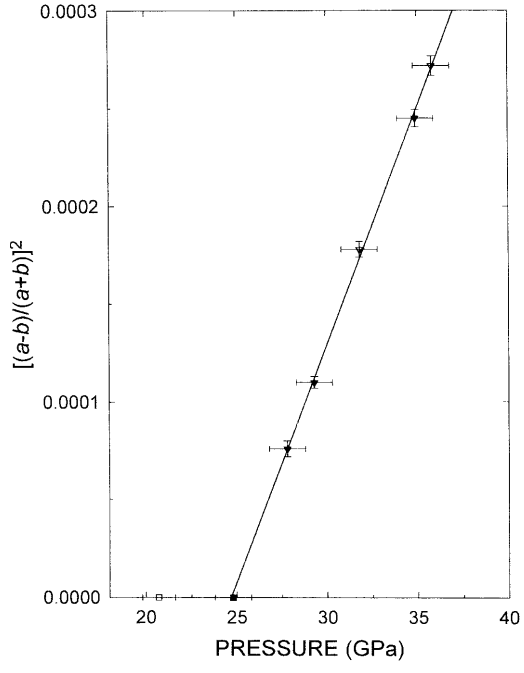

Fig. 6 Square of the spontaneous strain in rutile-type (□) and $CaCl_2$-type (▽) GeO_2 as a function of pressure. The *Line* represents a least-squares fit to the data. *Open* and *solid symbols* refer to points obtained on compression and decompression, respectively

GPa) yielded $B_0 = 241(10)$ GPa and $V/V_0 = 1.008(3)$ with B_0' fixed to 4. These values have no physical significance, as this phase is only present above the critical pressure of this second-order phase transition. The bulk modulus at P_c is 390(32) GPa for the rutile-type phase and 340(10) GPa for the $CaCl_2$-type phase. These results imply that the compressibility increases by 15% at the phase transition pressure. This increase in compressibility is predicted by Landau theory and can be understood in terms of the additional compression mechanism, polyhedral tilting, which is available in the orthorhombic phase. Alternatively, the data for both phases can be almost equally well fitted with a single equation of state with $B_0 = 262(6)$ GPa and $B_0' = 4.0(4)$. The present results are similar to those obtained for stishovite (Andrault et al. 1998), for which the B_0 of the $CaCl_2$-type phase of 282 GPa was found to be slightly lower than that of the rutile-type phase, 291 GPa; again the *P-V* data could alternatively be fitted to a single equation of state. A polyhedral bulk modulus (B_p) for the GeO_6 octahedron in the rutile-type phase was calculated to be 304(13) GPa with $B_p' = 8(2)$ using polyhedral volumes obtained from the data in Table 1 using the program IVTON (Balić-Žunić and Vicković 1996). The octahedron is thus 18% less compressible than the unit cell as a whole. Polyhedral volume calculations indicate that the octahedron is essentially incompressible above the phase transition at which polyhedral tilting becomes available as a compression mechanism.

The initial compressibilities of the rutile-type structure along **a** and **c** as obtained from a second-order polynomial fit to the data (Fig. 4; Table 2) are $\kappa_{a0} = 1.5(1) \times 10^{-3}$ GPa^{-1} and $\kappa_{c0} = 0.9(1) \times 10^{-3}$ GPa^{-1}. The κ_{a0}/κ_{c0} ratio is 1.7. The corresponding compressibilities of the rutile-type phase at the critical pressure of 25 GPa are $\kappa_{a25} = 1.0(2) \times 10^{-3}$ GPa^{-1} and $\kappa_{c25} = 0.5(2) \times 10^{-3}$ GPa^{-1}. An increase in the compressibility both in the *xy* plane and along **c** is observed at the phase transition [$\kappa_{(a+b)/2)25} = 1.1(1) \times 10^{-3}$ GPa^{-1} and $\kappa_{c25} = 0.7(1) \times 10^{-3}$ GPa^{-1}], Fig. 4, and the $\kappa_{(a+b)/2}/\kappa_c$ ratio is 1.5 above the transition. The overall compression in the *xy* plane is greater than that along the **c** direction in both phases, which is as expected as the columns of edge-sharing octahedra lie along **c**.

Table 2 Pressure dependence of the cell constants of rutile-type and $CaCl_2$-type GeO_2. Data were fitted to the following equation: $a = a_0 + a_1x + a_2x^2$, where $x = P$ for the rutile-type phase and $x = P - P_c$ for the $CaCl_2$-type phase. a_0 was fixed to the ambient value of the cell constant for the rutile-type phase and the value of the rutile-type phase at P_c for the $CaCl_2$-type phase

Cell constant	a_0 (Å)	a_1 (10^{-3} Å GPa^{-1})	a_2 (10^{-5} Å GPa^{-2})
Rutile			
a	4.3966	−6.6(5)	5.0(2.0)
c	2.8626	−2.5(3)	2.4(1.2)
$CaCl_2$			
a	4.2630	7.5(1.0)	−53(9)
b	4.2630	−17.8(1.8)	65(15)
c	2.8148	−2.1(1)	–
(*a* + *b*)/2	4.2630	−4.7(2)	–

Structural evolution of GeO_2 at high pressure

At ambient pressure, the GeO_6 octahedron is slightly elongated with two apical Ge-O distances of 1.905(1) Å and four equatorial distances of 1.871(1) Å. As was observed in the previous single-crystal X-ray diffraction study up to 3.7 GPa (Hazen and Finger 1981), the value of *x* decreases with increasing pressure. Consequently, the apical Ge-O distances compress to a greater extent than the equatorial distances and become shorter than the latter above 7 GPa (Fig. 7), yielding a flattened octahedron. This is easily understood, as the equatorial distances bridge the germanium atoms lying across the shared octahedral edge in the columns along **c**, whereas the apical distances participate in the cross-linkages in the compressible *xy* plane. The **c** lattice parameter corresponds to the shortest germanium-germanium distance in the structure. The next-shortest Ge-Ge distance lies along the [1 1 1] direction and is 19.6% longer at ambient pressure. The O-O distances decrease with pressure except for that corresponding to the short, shared octahedral edge, 2.409(2) Å at ambient pressure. This distance increases slightly both in the present study and the single-crystal work of Hazen and Finger (1981).

Robinson et al. (1971) defined two quantitative parameters to describe the distortion of polyhedra from

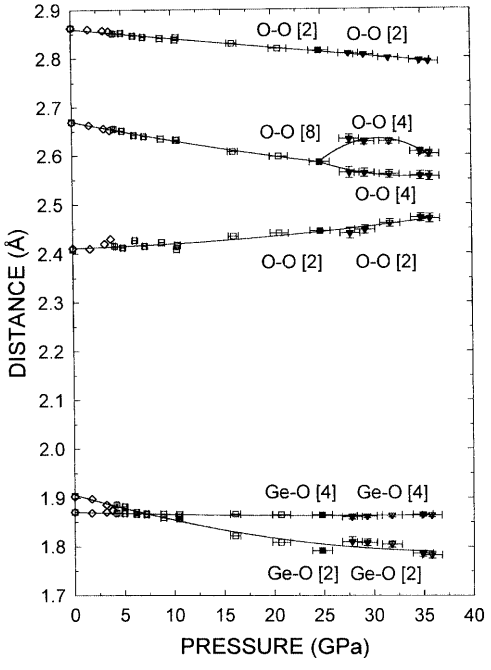

Fig. 7 Polyhedral interatomic distances in rutile-type (□) and $CaCl_2$-type (▽) GeO_2 as a function of pressure. The single-crystal data of Hazen and Finger 1981 are indicated by ◊. *Lines* represent least-squares fits to the data. *Open* and *solid symbols* refer to points obtained on compression and decompression, respectively. Bond multiplicities are given in *square brackets*

their ideal symmetries, angle variance, and quadratic elongation, which for an ideal polyhedron have values of 0 and 1, respectively. In rutile-type GeO_2, the angle variance decreases from 35.2 at ambient pressure to 23.5 at 25 GPa, while the quadratic elongation decreases from 1.010 to 1.007 over the same pressure range. The major part of the octahedral distortion is of angular origin as the O-Ge-O angles in the equatorial plane are of 99.84(3)° and 80.16(7)° at ambient pressure instead of the 90° expected for a regular octahedron. The respective values at 25 GPa are 98.0(1)° and 82.0(2)°. The overall effect of pressure is to slightly reduce the polyhedral distortion in the GeO_6 octahedra.

The transition, as expected from the high polyhedral bulk modulus of the GeO_6 octahedron, has little effect on the apical and equatorial Ge-O distances, which are 1.792(3) Å and 1.864(2) Å at 25(1) GPa and 1.81(1) Å and 1.86(1) Å at 28(1) GPa. There is also very little effect on the intrapolyhedral O-Ge-O angles. The O-Ge-O angles in the equatorial plane of the octahedron continue their gradual progression towards 90° reaching 97.0(2)° and 83.0(4)° by 36 GPa. At this pressure the other O-Ge-O angles, which in the $CaCl_2$-type structure are no longer required by symmetry to be 90°, deviate by only 1°. Consequently, the distortion parameters further decrease with the angle variance and quadratic elongation reaching 18.6 and 1.006, respectively.

The columns of edge-sharing octahedra are permitted by symmetry to tilt about their two fold axes above the phase transition. Bärninghausen and coworkers (Bärninghausen et al. 1984; Range et al. 1987) described the rotation of the columns of octahedra with respect to their original orientation in the rutile-type structure in terms of two angles ω and ω', where:

$$\mathrm{Tan}(45^\circ + \omega) = b(1/2 - y)/a(1/2 - x) \quad (2)$$

and

$$\mathrm{Tan}(45^\circ - \omega') = by/ax \ , \quad (3)$$

with a and b being the cell constants and x and y the oxygen coordinates for the $CaCl_2$-type structure. The angles ω and ω' in $CaCl_2$-type GeO_2 were found to increase up to 10.2(5)° and 8.6(3)°, respectively, at 36(1) GPa, so as to yield a hexagonal close-packed oxygen sublattice (Fig. 1). These values are comparable to the 11.91° and 8.00° observed for β-PtO_2 (Range et al. 1987), which is the only $CaCl_2$-type dioxide which can be recovered and studied at ambient pressure. In the present case, the MO_6 octahedra are slightly less distorted. The tilting of the highly incompressible octahedra, $B_p = 304(13)$ GPa, is favored by the application of pressure, as this compression mechanism produces a hexagonal close-packed (hcp) oxygen sublattice and, consequently, a denser structure. A tilt angle of 10°, in fact, places the oxygens, which initially form buckled layers in the disorted puckered hexagonal close-packed array (tetragonal close packing) of the rutile-type structure, in planar layers corresponding to hexagonal close packing (Baur 1994).

Systematic relationships in the group 14 dioxides

The present investigation of rutile-type GeO_2 permits a comparison to be made with recent data for isotypic stishovite, SnO_2, and PbO_2 in order that systematic behavior can be identified. Considerable work has been done on bulk modulus volume systematics, in particular that of Anderson (1972), which yielded the following relationship:

$$B_0 = 700\, S^2 Z_A Z_C / V_0 \ , \quad (4)$$

where S^2 is the ionicity, $S^2 = 0.5$ for oxides, Z_A and Z_C are the formal anion and cation charges, respectively, and V_0 is the molar volume per ion pair. This relationship gives the following B_0 values for the group-14 dioxides when going from Si to Pb: 299 GPa, 252 GPa, 195 GPa, and 168 GPa. The experimental values for stishovite, 298(8) GPa (Hemley et al. 1994), and the present value of 250(9) GPa for rutile-type GeO_2 are in very good agreement with these values obtained from this systematic relationship. Similarly, the bulk moduli of 205(7) and 176(16) GPa obtained for SnO_2 (Haines and Léger 1997) and PbO_2 (Haines et al. 1996a), respectively, are in relatively good agreement.

The polyhedral bulk moduli also vary with the inverse of the polyhedral volume. The bulk modulus of the SiO_6 octahedron in stishovite was found from single-crystal, X-ray diffraction at high pressure to be 342 GPa (Ross et al. 1990). If this value is multiplied by the ratio of polyhedral volumes, one can calculate the following values for GeO_6, 287 GPa, and for SnO_6, 223 GPa. The experimental polyhedral bulk moduli are, respectively, 304(13) GPa and 209–243 GPa, depending on the value of the first pressure derivative. These polyhedral bulk moduli thus scale well to the value obtained for stishovite. It can be seen for these dioxides that the compression of both the unit cell and the constituent polyhedra varies systematically, indicating that these structures respond in a very similar way to applied pressure.

The ratio of the compressibilities along **a** and **c**, κ_{a0}/κ_{c0}, in the series SiO_2, GeO_2, SnO_2 is essentially constant with values of 1.8 (Ross et al. 1990), 1.7, and 1.9 (Haines and Léger 1997), respectively. In all cases, the chain direction is thus significantly less compressible with respect to compression in the xy plane.

The oxygen x-coordinate was found to decrease as a function of pressure in SiO_2, GeO_2, and SnO_2 and, as a consequence, in all three dioxides the two apical M-O distances lying in the xy plane decrease to a greater extent than the four equatorial distances, which bridge the cations along the chain direction The former distances become shorter than the latter at 7 GPa in GeO_2. The pressure at which this occurs in stishovite is 35 GPa upon extrapolating the single-crystal results of Ross et al. (1990), and around 54 GPa based on the powder work of Andrault et al. (1998). These apical and equatorial distances in SnO_2 are very similar at ambient pressure, with recent data indicating that the apical

distances are shorter (Bolzan et al. 1997). The apical distances also decrease to a greater extent than the equatorial distances at high pressure (Haines and Léger 1997). The apical distances are shorter in PbO_2 at ambient pressure (Hill 1982). The type of tetragonal distortion (two short distances–four long distances) observed for SnO_2 and PbO_2 is that predicted by a simple ionic model (Baur 1961), which is also observed for rutile-type metal difluorides and a number of other metal dioxides. It has been proposed that the opposite type of distortion (two long distances–four short distances) observed for some smaller cation dioxides is mainly due to anion-anion repulsions (Burdett 1985, 1995). It is apparent that at high pressure cation-cation repulsions predominate and, as a consequence, above given pressures, SiO_2 and GeO_2 exhibit the same type of distortion as that observed for SnO_2 and PbO_2.

The critical pressure for the rutile-type to $CaCl_2$-type phase transitions in SiO_2, GeO_2, and SnO_2 was found to be a linear function of the square of the frequency of the B_{1g} soft mode at ambient pressure with $P_c = 9.886 \times 10^{-4} v_{B1g}^2 - 2.8$ (Haines et al. 1998). It is this mode, involving the libration of the columns of MO_6 octahedra, which drives the phase transition. Above the rutile-type to $CaCl_2$-type phase transition, the rotation angle of the columns of octahedra was found to rapidly approach 10° in GeO_2 and SnO_2, thereby producing a hexagonal close-packed oxygen array. In contrast, the rotation angle in $CaCl_2$-type SiO_2 was not found to increase beyond 6° up to 120 GPa (Andrault et al. 1998).

The rutile-type to $CaCl_2$-type phase transition and the resulting formation of an hcp oxygen sublattice can be considered as a first step in pathways towards denser structure types such as α-PbO_2 and Fe_2N. Transitions to these denser phases occur at pressures similar to those at which the rutile to $CaCl_2$ transitions are observed (Table 3). The $CaCl_2$-, α-PbO_2-, and Fe_2N-type structures are all based on an hcp oxygen sublattice, with half the octahedral sites occupied by cations. The $CaCl_2$- and α-PbO_2-type structures represent different cation-ordering patterns and in the Fe_2N(L′3)-type structure the cation sites are randomly occupied (Liu et al. 1978). Transformation between these structures requires significant energy, as cation displacements are necessary. The $CaCl_2$-type phases in the group-14 dioxides either exhibit a limited pressure range of stability or are metastable, as in the case of PbO_2, and their occurrence is an indication of the proximity of a further transition to a denser phase; however, as there is a very high energy barrier between the $CaCl_2$-type structure and these denser structures, their formation requires high temperature or shear stress and, in the case of SiO_2 and GeO_2, the use of low-density vitreous or quartz-type starting materials. Further transitions to much denser cubic, $Pa\bar{3}$-modified-flourite-type phases are predicted from theoretical calculations for SiO_2(Park et al. 1988; Cohen 1992; Dubrovinsky et al. 1997; Teter et al. 1998) and GeO_2 (Jolly et al. 1994), and have been observed experimentally for SnO_2 and PbO_2 (Haines et al. 1996b). The group-14 dioxides thus undergo one or more steps along the following high-pressure phase-transition sequence: rutile → $CaCl_2$ and/or Fe_2N and/or α-PbO_2 → $Pa\bar{3}$.

Table 3 Ambient-temperature pressures (GPa) for transitions to postrutile phases in group-14 dioxides[a]

	$CaCl_2$	α-PbO_2[b]	Fe_2N[b]	$Pa\bar{3}$
SiO_2	50c, 54e[b], 56b	68d	35–40a	–
GeO_2	25h[b]–26.7g	–	25–30a, f	–
SnO_2	11.8j	14i	–	21j
PbO_2	4l	1k	–	7l

[a] Data from the following references: SiO_2 – (a, Liu et al. 1978; b, Mao et al. 1994; c, Kingma et al. 1995; d, Dubrovinsky et al. 1997; e, Andrault et al. 1998). GeO_2 – (a, Liu et al. 1978; f, Ming and Manghnani 1983; g, Haines et al. 1998; h, this work). SnO_2 – (i, Suito et al. 1975; j, Haines and Léger 1997); PbO_2 – (k, White et al. 1961; l, Haines et al. 1996a)

[b] Based on the study of heated samples

Conclusions

The structural evolution of rutile-type and $CaCl_2$-type GeO_2 has been investigated at high pressure. The phase transition from the tetragonal rutile-type phase to the orthorhombic $CaCl_2$-type phase is shown to be second-order and proper ferroelastic. Compression of the GeO_6 octahedron is anisotropic, with the apical Ge-O distances shortening to a much greater extent than the equatorial distances. This modifies the type of tetragonal distortion observed for the octahedron, and at pressures above 7 GPa, the type of distortion present is the same as that observed for SnO_2 and PbO_2. Above the phase transition, the columns of edge-sharing GeO_6 octahedra tilt about their two fold axes so as to yield an hcp oxygen sublattice. Systematic relationships are identified in the group-14 dioxides, which arise from the strong similarities in their structures and vibrational properties.

References

Anderson OL (1972) Patterns in elastic constants of minerals important to geophysics. In: Robertson EC (ed) The nature of the solid earth. McGraw-Hill, New York, pp 575–613

Andrault D, Fiquet G, Guyot F, Hanfland M (1998) Pressure-induced Landau-type transition is stishovite. Science 282: 720–724

Balić-Žunić T, Vicković I (1996) IVTON – a program for the calculation of geometrical aspects of crystal structures and some crystal chemical applications. J Appl Crystallogr 29: 305–306

Bärninghausen H, Bossert W, Anselment B (1984) A second-order phase transition of calcium bromide and its geometrical interpretation. Acta Crystallogr A40: C-96

Baur WH (1961) Uber die Verfeinerung der Kristallstrukturbestimmung einiger Vertreter des Rutiltyps. III. Zur Gittertheorie des Rutiltyps. Acta Crystallogr 14: 209–213

Baur WH (1981) A three-dimensional periodic, 11-coordinated, dense packing of symmetry equivalent spheres. Mater Res Bull 16: 339–345

Baur WH (1994) Rutile-type derivatives. Z Kristallogr 209: 143–150

Baur WH, Khan AA (1971) Rutile-type compounds. IV. SiO_2, GeO_2 and a comparison with other rutile-type structures. Acta Crystallogr B27: 2133–2139

Birch F (1947) Finite elastic strain of cubic crystals. Phys Rev 71: 809–824

Bolzan AA, Fong C, Kennedy BJ, Howard CJ (1997) Structural studies of rutile-type metal dioxides. Acta Crystallogr B53: 373–380

Burdett JK (1985) Electronic control of the geometry of rutile and related structures. Inorg Chem 24: 2244–2253

Burdett JK (1995) Structural-electronic relationships in rutile. Acta Crystallogr B51: 547–558

Chang R, Graham LJ (1966) Low-temperature elastic properties of ZrC and TiC. J Appl Phys 37: 3778–3783

Cohen RE (1992) First-principles predictions of elasticity and phase transitions in high pressure SiO_2 and geophysical implications. In: Syono Y, Manghnani MH (eds) High-pressure research: applications to earth and planetary sciences. TERRAPUB/Am Geophys Union, Washington, DC, pp 425–431

Dubrovinskaia NA, Dubrovinsky LS, Saxena SK, Ahuja R, Johansson B (1999) High-pressure study of titanium carbide. J Alloys Compounds 289: 24–27

Dubrovinsky LS, Saxena SK, Lazor P, Ahuja R, Eriksson O, Wills JM, Johansson B (1997) Experimental and theoretical identification of a new high-pressure phase of silica. Nature 388: 362–365

Haines J, Léger JM (1993) Phase transitions in ruthenium dioxide up to 40 GPa: mechanism for the rutile-to-fluorite phase transformation and a model for the high-pressure behavior of stishovite SiO_2. Phys Rev B 48: 13344–13350

Haines J, Léger JM (1997) X-ray diffraction study of the phase transitions and structural evolution of tin dioxide at high pressure: relationship between structure types and implications for other rutile-type dioxides. Phys Rev B 55: 11144–11154

Haines J, Léger JM, Hoyau S (1995) Second-order rutile-type to $CaCl_2$-type phase transition in β-MnO_2 at high pressure. J Phys Chem Sol 56: 965–973

Haines J, Léger JM, Schulte O (1996a) The high-pressure phase transition sequence from the rutile-type through to cotunnite-type structure in PbO_2. J Phys: Condens Matter 8: 1631–1646

Haines J, Léger JM, Schutle O (1996b) $Pa\bar{3}$ modified fluorite-type phases in metal dioxides at high pressure. Science 271: 629–631

Haines J, Léger JM, Schulte O, Hull S (1997) Neutron diffraction study of the ambient-pressure, rutile-type and the high-pressure $CaCl_2$-type phases of ruthenium dioxide. Acta Crystallogr B53: 880–884

Haines J, Léger JM, Chateau C, Bini R, Ulivi L (1998) Ferroelastic phase transition in rutile-type germanium dioxide at high pressure. Phys Rev B 58: R2909–R2912

Hazen RM, Finger LW (1981) Bulk moduli and high-pressure crystal structures of rutile-type compounds. J Phys Chem Sol 42: 143–151

Hemley RJ, Prewitt CT, Kingma KJ (1994) High-pressure behavior of silica. Rev Mineral 29: 41–81

Hill RJ (1982) The crystal structures of lead dioxides from the positive plate of the lead/acid battery. Mater Res Bull 17: 769–784

Jolly LH, Silvi B, D'Arco P (1994) Periodic Hartree-Fock study of minerals: hexacoordinated SiO_2 and GeO_2 polymorphs. Eur J Mineral 6: 7–16

Kingma KJ, Cohen RE, Hemley RJ, Mao HK (1995) Transformation of stishovite to a denser phase at lower-mantle pressures. Nature 374: 243–245

Léger JM, Haines J, Pereira AS (1998) Structural investigations under high pressure. Rev High Pressure Sci Technol 7: 295–297

Liu LG, Bassett WA, Sharry J (1978) New high-pressure modifications of GeO_2 and SiO_2. J Geophys Res 83: 2301–2305

Mao HK, Xu J, Bell PM (1986) Calibration of the ruby pressure gauge to 800 kbar under quasi-hydrostatic conditions. J Geophys Res 91: 4673–4676

Mao H, Shu J, Hu J, Hemley RJ (1994) Single-crystal X-ray diffraction of stishovite to 65 GPa. EOS Trans Am Geophys Union, Washington, DC, 75: 662

Ming LC, Manghnam MH (1983) High-pressure phase transformations in vitreous and crystalline GeO_2 (rutile). Phys Earth Planet Inter 33: 26–30

Park KT, Terakura K, Matsui Y (1988) Theoretical evidence for a new ultra-high-pressure phase of SiO_2. Nature 336: 670–672

Range KJ, Rau F, Klement U, Heyns AM (1987) β-PtO_2: high pressure synthesis of single crystals and structure refinement. Mater Res Bull 22: 1541–1547

Robinson K, Gibbs GV, Ribbe PH (1971) Quadratic elongation: a quantitative measure of distortion in coordination polyhedra. Science 172: 567–570

Ross NL, Shu JF, Hazen RM, Gasparik T (1990) High-pressure crystal chemistry of stishovite. Am Mineral 75: 739–747

Salje EKH (1990) Phase transitions in ferroelastic and co-elastic crystals. Cambridge University Press, Cambridge

Stokes HT, Hatch DM (1998) Isotropy subgroups of the 230 crystallographic space groups. World Scientific, Singapore

Suito K, Kawai N, Masuda Y (1975) High pressure synthesis of orthorhombic SnO_2. Mater Res Bull 10: 677–680

Teter DM, Hemley RJ, Kresse G, Hafner J (1998) High pressure polymorphism in silica. Phys Rev Lett 80: 2145–2148

Tsuchiya T, Yamanaka T, Matsui M (1998) Molecular dynamics study of the crystal structure and phase, relation of the GeO_2 polymorphs. Phys Chem Miner 25: 94–100

Wang H, Simmons G (1973) Elasticity of some mantle crystal structures. II. Rutile GeO_2. J Geophys Res 78: 1262–1273

Wells AF, Chamberland BL (1987) Relations between dense sphere packings. J Solid State Chem 66: 26–39

West AR, Bruce PG (1982) Tetragonal-packed crystal structures. Acta Crystallogr B38: 1891–1896

White WB, Dachille F, Roy R (1961) High-pressure-high-temperature polymorphism of the oxides of lead. J Am Ceram Soc 44: 170–174